biomolecules

MDPI

Article

Proteasome Inhibition Is an Effective Treatment Strategy for Microsporidia Infection in Honey Bees

Emily M. Huntsman [1,†], Rachel M. Cho [1,†], Helen V. Kogan [1], Nora K. McNamara-Bordewick [1], Robert J. Tomko, Jr. [2] and Jonathan W. Snow [1,*]

[1] Biology Department, Barnard College, New York, NY 10027, USA; emh2237@barnard.edu (E.M.H.); rmc2201@barnard.edu (R.M.C.); lena.vkogan@gmail.com (H.V.K.); noramcb@gmail.com (N.K.M.-B.)
[2] Department of Biomedical Sciences, Florida State University College of Medicine, Tallahassee, FL 32306, USA; robert.tomko@med.fsu.edu
* Correspondence: jsnow@barnard.edu; Tel.: +1-212-854-2084
† These authors contributed equally to this work.

Abstract: The microsporidia *Nosema ceranae* is an obligate intracellular parasite that causes honey bee mortality and contributes to colony collapse. Fumagillin is presently the only pharmacological control for *N. ceranae* infections in honey bees. Resistance is already emerging, and alternative controls are critically needed. *Nosema* spp. exhibit increased sensitivity to heat shock, a common proteotoxic stress. Thus, we hypothesized that targeting the *Nosema* proteasome, the major protease removing misfolded proteins, might be effective against *N. ceranae* infections in honey bees. *Nosema* genome analysis and molecular modeling revealed an unexpectedly compact proteasome apparently lacking multiple canonical subunits, but with highly conserved proteolytic active sites expected to be receptive to FDA-approved proteasome inhibitors. Indeed, *N. ceranae* were strikingly sensitive to pharmacological disruption of proteasome function at doses that were well tolerated by honey bees. Thus, proteasome inhibition is a novel candidate treatment strategy for microsporidia infection in honey bees.

Keywords: *Nosema ceranae*; microsporidia; proteasome; therapeutic; pollination

Citation: Huntsman, E.M.; Cho, R.M.; Kogan, H.V.; McNamara-Bordewick, N.K.; Tomko, R.J., Jr.; Snow, J.W. Proteasome Inhibition Is an Effective Treatment Strategy for Microsporidia Infection in Honey Bees. *Biomolecules* **2021**, *11*, 1600. https://doi.org/10.3390/biom11111600

Academic Editor: Shigeo Murata

Received: 27 September 2021
Accepted: 26 October 2021
Published: 29 October 2021

1. Introduction

The western honey bee, *Apis mellifera*, provides pollination services of critical importance to humans in both agricultural and ecological settings [1]. Honey bee colonies have suffered from increased mortality in recent years that is likely caused by a complex set of interacting stresses [2]. Among the environmental stressors linked to honey bee disease, there has been intensifying focus on the role of microbial attack on honey bee health [3]. The microsporidian species *Nosema ceranae* and *Nosema apis* can cause individual mortality in honey bees and have been implicated in colony collapse [4–6]. *N. apis* has been a well-appreciated pathogen of *A. mellifera* for a century. *N. ceranae*, which originated in the eastern honey bee, *Apis cerana*, was first observed in *A. mellifera* in the early 2000s and appears to have displaced *N. apis* in the western honey bee in many regions [5,6]. *N. ceranae*, an obligate intracellular parasite, is now one of the most common pathogens of the honey bee. Midgut infection by this unicellular eukaryote causes energetic stress, epithelial damage, and when untreated, death [7–12]. Furthermore, infection is associated with a number of physiological and behavioral changes that likely affect individual contribution to the colony [10,11,13–15].

In the United States, *N. ceranae* infection has traditionally been controlled by treatment with the drug fumagillin. However, its use is prohibited in Europe (reviewed in [16]) and its effectiveness in controlling *N. ceranae* at the colony level appears limited in scope and duration [17]. Equally troubling, high doses of this drug impact host cell function and evidence suggests that *N. ceranae* can evade suppression in some circumstances [18].

Critically, future availability of fumagillin is also uncertain due to production, safety, and market issues. Thus, efforts to find new treatment strategies are critical to protect honey bees from this parasite [16,19]. Many promising alternatives strategies for control of *N. ceranae* infection have now been pursued, including important studies exploring other small molecules, RNAi, probiotics, and various natural compounds ([20–29] and work prior to 2020 reviewed in [30]). Eukaryotic pathogens can be challenging to combat using chemical antimicrobials because of the phylogenetic closeness with their hosts, and microsporidia are no exception. However, comparative genomics indicates that microsporidia have lost many of the cellular processes and pathways found in free-living eukaryotes [31], perhaps suggesting a loss of the redundancy and flexibility that often allows organisms to withstand cellular stresses. In support of this, fumagillin, as a methionine aminopeptidase 2 inhibitor, works by interfering with protein synthesis, thereby disrupting protein homeostasis, or the homeostasis of protein synthesis, folding, function, and degradation. In addition to sensitivity to fumagillin, *N. ceranae* exhibit vulnerability to other proteotoxic stresses, including thermal stress, which we previously confirmed in parallel with characterization of the response to heat shock in this species [32], and tRNA synthetase inhibition [33]. The regulated clearance of proteins is another aspect of protein homeostasis that is critical to the functionality of the proteome [34,35]. This process is mediated by a number of pathways including degradation by the ubiquitin–proteasome system (UPS) [36].

The UPS is a complex system that targets proteins for regulated degradation in an energy-dependent manner. Proteins to be destroyed are typically first covalently modified with a chain of the small protein ubiquitin, which serves as a signal for recognition by the proteasome. The proteasome is a large, multi-subunit, ATP-dependent protease complex that cleaves substrates into short peptides and recycles the polyubiquitin targeting signal. In addition to the clearance of damaged or misfolded proteins, the proteasome also serves an important regulatory function by destroying signaling proteins involved in various cellular processes.

The archetypal 26S proteasome is made up of a barrel-shaped core 20S proteolytic complex known as the core particle (CP) and one or two 19S regulatory particles (RP) that cap the barrel ends. The RP can be biochemically divided into two subcomplexes, the lid and the base [37,38]. The base contains six AAA+ family ATPase subunits, Rpt1-6, and three non-ATPase subunits, Rpn1, Rpn2, and Rpn13. The lid consists of nine non-ATPase subunits, Rpn3, Rpn5-9, Rpn11, Rpn12, and Rpn15/Sem1. One additional subunit, Rpn10, associates with the otherwise fully assembled RP and contacts both the lid and the base.

The RP is responsible for initial substrate capture via the ubiquitin-binding activities of Rpn1, Rpn10, or Rpn13. Once the substrate is captured, the polyubiquitin chain is removed by an intrinsic deubiquitinating activity within the Rpn11 lid subunit, and the substrate is unfolded via ATP-dependent mechanical motions of the ATPases Rpt1-6. The unfolding process also translocates the substrate into the center of the CP barrel for proteolysis. The CP consists of four axially stacked heteroheptameric rings of 7 α subunits or 7 β subunits. The α rings are responsible for interfacing with the RP and controlling access to the peptidase sites, whereas the proteolytic activity is housed within the β rings and is mediated by three of the β subunits (β1, β2, and β5). The β1, β2, and β5 subunits are referred to as caspase-like, trypsin-like, and chymotrypsin-like, based on their cleavage preferences [36].

As a sensitivity of microsporidia to UPS disruption might also be expected due to their compacted genomes, we examined genes associated with the UPS in *N. ceranae* and found that this species has a degenerate proteasome apparently lacking multiple components observed in most eukaryotes. However, based on sequence analysis and structural modeling of the key catalytic subunit, β5, proteasome inhibitors were predicted to disrupt function. In agreement with this supposition, we observed a striking sensitivity of *N. ceranae* to pharmacological disruption of proteasome function without a concomitant reduction in honey bee survival, suggesting the possibility of exploring proteasome inhibitors as novel anti-Nosema chemical agents.

2. Materials and Methods

2.1. Honey Bee Colonies and Caging Experiments

Honey bees were collected from outbred colonies in New York, New York consisting of a typical mix of *Apis mellifera* subspecies found in North America, at different times during the months of April–October. Source colonies were visually inspected for symptoms of common bacterial, fungal, and viral diseases of honey bees. For caging experiments, bees were collected from the landing board or newly emerged bees were collected after hatching from a capped brood frame overnight in an incubator at 35 °C in the presence of Pseudo-Queen (Contech, Victoria, British Columbia, Canada) as a source of Queen Mandibular Pheromone (QMP). Approximately 20 landing board bees or 30 newly eclosed bees were placed in each 4.8 × 3.4 × 8.4 inch acrylic cage with sliding door machined at Carelton Labs, Columbia University. For cages containing newly eclosed bees, approximately 4 foragers from the same source colony (marked with a spot of paint (Testors, Vernon Hills, IL, USA) were added to each cage. Caged bees were maintained in incubators at 35 °C (unless otherwise stated) in the presence of PseudoQueen (Contech, Victoria, BC, Canada) as a source of Queen Mandibular Pheromone (QMP).

2.2. Nosema ceranae Spore Isolation and Quantification

N. ceranae spores were obtained from infected individuals for use in infection studies [8,39]. In addition, an isolate was obtained from this colony and serially passaged through bees as performed previously [40]. Spores from these bees were used in most experiments. The species of Nosema used for infection was verified by qPCR. To isolate spores, midguts from infected or uninfected bees were individually crushed in 0.5 mL H20 and spore number was assessed by light microscopy. Midguts were washed 3 times with water and resuspended in 33% sucrose solution at a concentration of 1×10^6 spores per mL for landing board bees or 5×10^6 spores per mL for newly eclosed bees.

2.3. Nosema ceranae Infections and Chemical Treatments

For experiments with landing board bees, caged bees were allowed to consume food containing spores ad libitum for 24 h before food was replaced with sucrose solution alone. Bees in the uninfected group always received sucrose solution containing a midgut from an uninfected bee processed in the same way as the midgut containing spores. For experiments with newly emerged bees, caged bees were fed sucrose solution and supplied with a ~5 g pollen substitute patty (1:1 mix of BeePro and sucrose solution). On day 2 post-eclosion, *N. ceranae* spores (5×10^6/mL) were fed to bees in sucrose solution ad libitum [41] for 48 h. At 3 days post infection, honey bees in individual cages (landing board bees and newly eclosed bees) were fed sucrose solution containing one of the pharmacologic agents (Supplemental Table S4) or vehicle control alone (DMSO) at the indicated doses. After 4 days of drug feeding, honey bee midguts were dissected, crushed in 0.5 mL water, and the number of mature spores counted by light microscopy as previously described [41]. In parallel, qPCR was used to determine relative amount of *N. ceranae* genome equivalents versus host genome equivalents.

For survival experiments, newly eclosed bees were caged and fed as above, but were left uninfected. Starting on 4 days post eclosion, bees were switched to sucrose solution containing one of the pharmacologic agents (Supplemental Table S4) or vehicle control alone (DMSO) at the indicated dose for 10 days while survival was assessed.

2.4. DNA Extraction and qPCR

DNA extraction was performed using a modified Smash and Grab DNA Miniprep protocol as described previously [42]. The resulting DNA was used as a template for qPCR to determine the levels infection for *Nosema* sp. using primer sequences for the *N. apis 16S* gene, the *N. ceranae β-actin* gene, and the honey bee *ATP5a* gene [42]. Reactions were performed with PowerUp SYBR Green Master Mix (Applied Biosystems, Foster City, CA, USA) in a LightCycler 480 thermal-cycler (Roche, Branchburg, NJ, USA). The difference

between the threshold cycle (Ct) number for honey bee *ATP5a* and that of the *Nosema* sp. gene of interest was used to calculate the relative infection level using the $\Delta\Delta C_T$ method. A sample was considered negative for a specific *Nosema* species if it did not amplify any product by 35 cycles and zero was entered as the value in these cases.

2.5. Ortholog Screening of the N. ceranae and Other Microsporidian Genomes

The KEGG (Kyoto Encyclopedia of Genes and Genomes) database was used as a guide for comparing pathways between species [43]. In addition to looking at proteasome pathway gene candidates predicted by this database (nce03050), pathway genes from *S. cerevisiae* (sce03050) were used to find orthologs in the *N. ceranae* genome as well as other available microsporidian genomes using the BLAST family of search functions (www.ncbi.nlm.nih.gov (accessed on 12 August 2020)) as described previously [44]. Coding sequences from human or other eukaryotes were also used as queries to further support the absence of selected genes from microsporidian genomes.

2.6. CP α Subunit Ortholog Assignment and N. ceranae α Ring Homology Model Generation

After unsuccessful assignment of α subunit orthologs by pairwise comparison to human and *S. cerevisiae* genomes using BLAST, a protein threading approach guided by secondary structure and residue exposure was utilized. Specifically, the CPHmodels 3.2 server (http://www.cbs.dtu.dk/services/CPHmodels/ (accessed on 12 August 2020)) was used to identify best templates and to generate PDB models of each *N. ceranae* α subunit. The best-fit model in each case confidently identified a specific α subunit (E: $<10^{-20}$), except for XP_024331661.1, which yielded a low-confidence fit to *B. taurus* α2 from PDB ID 1IRU. Remote homology modeling using the *T. acidophilum* α subunit yielded a high-confidence homology model for this protein. Considering the high-confidence identification of homologs for the other six subunits (α2–α7) using this approach, we tentatively assigned XP_024331661.1 as α1.

We next assembled a homology model of the α ring by superimposing each subunit onto its ortholog in the *S. cerevisiae* CP crystal structure (PDB ID = 1RYP) using Pymol 1.3r1 (Schrödinger, Inc. New York, NY, USA.This yielded a model with little to no apparent steric conflict. In the model, a lysine residue was positioned appropriately in each α-α interface for salt bridging with Rpt subunit C-termini as reported for the Archaeal, yeast, and human proteasomes (note that α7 contains a conservative arginine substitution at this position instead of a lysine). Importantly, the pocket formed by α7 and our tentative α1 subunit lacked a lysine residue contributed by α1 for salt bridging, which is a conserved feature of the CP from other eukaryotes. Finally, assuming the arrangement of Rpt subunits and the register of the RP relative to the CP is conserved in the *N. ceranae* RP, the resultant model would align the lone Rpt tail that lacks a Hb-Y-X motif, Rpt4, with the lysineless α7-α1 pocket as observed in other eukaryotic CPs. These observations further supported the assignment of XP_024331661.1 as *N. ceranae* α1.

2.7. Molecular Modeling of the N. ceranae β5-Ixazomib Complex

A homology model of *N. ceranae* β5 was generated using CPHmodels 3.2 as above. The model was then superimposed on chain b of the crystal structure of ixazomib bound to the human CP (PDB ID = 5LF7) using the "align" command in Pymol, yielding a fit with RMSD = 1.567 Å. Steric clash was assessed via visual inspection and conservation of salt bridging or hydrogen bonding was inferred from inter-atom spacing of $\leq$4 Å.

2.8. Statistical Analysis

Data is presented as means ± SEM shown. For two groups, data was compared using unpaired t-tests with Welch's correction when values fit normal distributions or Mann–Whitney U nonparametric tests when they did not fit normal distributions. Normality was assessed using Shapiro–Wilk tests. When more than two groups were being compared, data was compared using one-way ANOVA with Tukey's multiple comparison test when values

fit normal distributions or a Kruskall–Wallis test when they did not. For survival analysis, treated versus untreated groups were compared using the Gehan–Breslow–Wilcoxon test.

3. Results

3.1. N. ceranae Lack Obvious Orthologs of Several Proteasome Subunits, Proteasomal Assembly Chaperones, and the Proteasome Regulatory Transcription Factor Rpn4

Using *Saccharomyces cerevisiae* proteins as queries [45], we searched for proteasome components in a number of disparate microsporidia genomes, including *N. ceranae*, *N. apis*, *Encephalitozoon hellem*, *Nematocida displodere*, and *Mitosporidium daphnia* (which represents an early diverging microsporidian species that does not demonstrate the genome compaction observed in other microsporidia [46]). We also examined proteasome components in *Rozella allomycis*, which is a member of the *Cryptomycota* group that is closely related to microsporidia [46], and three other fungal species, *Candida albicans*, *Aspergillus fumigatus*, and *Schizosaccharomyces pombe*.

First, we searched for proteins making up the RP. Although obvious homologs of most RP subunits could be identified in each species, we were unable to find orthologs of the lid subunits Rpn3, Rpn12, and Rpn15/Sem1 or the base subunit and ubiquitin receptor Rpn13 in any of the species examined (Figure 1, Supplemental Table S1 and Video S1). Use of other fungal or mammalian orthologs as queries also failed to yield any homologs. Alignment of RP subunit protein sequences from *N. ceranae* with those of *S. cerevisiae*, whose proteasome has been visualized at near-atomic resolution [47–53], revealed that the enzymatic subunits of the RP (Rpn11 and the six Rpt subunits) have the highest overall sequence identity to that of *S. cerevisiae*, particularly within the catalytic domains (Figure 1; Supplemental Video S1). A notable feature with respect both to lid and base subunits was the truncation of selected N- and C-termini of the *N. ceranae* subunits. Prominent among these truncations were the N-termini of lid subunits Rpn5, Rpn6, and Rpn7. In yeast and other eukaryotes, the N-termini of these subunits make critical contacts with the CP and/or the ATPase ring of the base [54–57], raising the possibility that communication between these subcomplexes may be altered in microsporidia. Alterations in the lengths or sequences of lid subunits that create a key helical bundle critical for assembly and stability of the lid were also evident; these likely evolved to accommodate the absence of Rpn3, Rpn12, and Rpn15/Sem1, which have key roles in the assembly and stability of the lid in yeast [58–61].

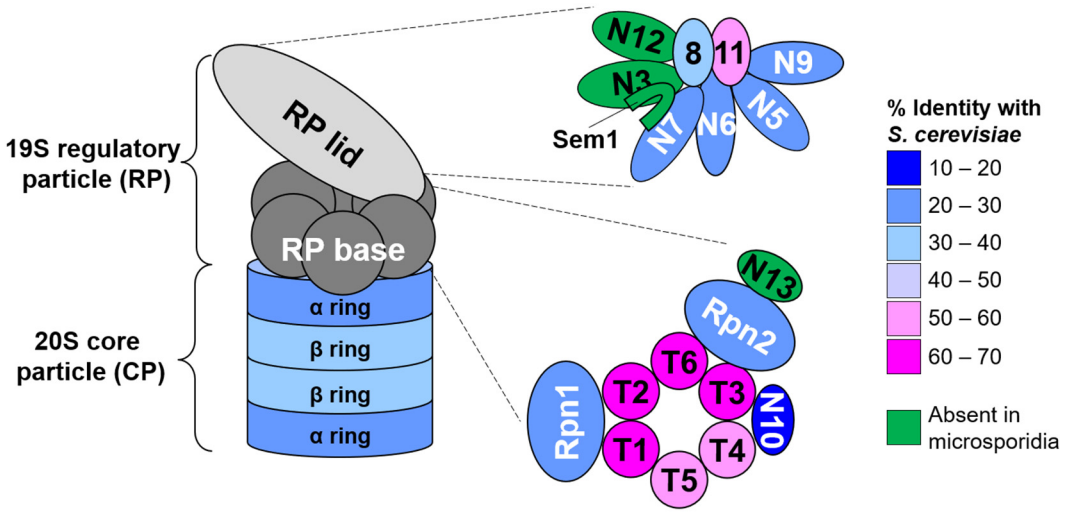

Figure 1. Ultrastructure and conservation of the *N. ceranae* 26S proteasome. Cartoon model of the canonical 26S proteasome. The 19S regulatory particle (RP) consists of lid and base subcomplexes. Detailed subunit compositions are shown to the right. The 20S core particle (CP) consists of four stacked heteroheptameric rings of α and β subunits. The coloring of the subunits indicates their sequence identity with their respective *S. cerevisiae* orthologs. For the CP, the average sequence identity of the seven subunits is displayed. Subunits shown in green appear to be absent from *N. ceranae* and all other microsporidia examined.

Within the base, the N-termini of several Rpt subunits were truncated somewhat compared to their *S. cerevisiae* orthologs, but the significance of this is not immediately evident. Overall, the non-ATPase subunits Rpn1 and Rpn2 displayed the least sequence conservation with that of *S. cerevisiae* (~22% identity each vs. ~60% for each Rpt subunit). Further, key functional regions of both subunits were absent. These included a number of residues within Rpn1 responsible for ubiquitin binding in the *S. cerevisiae* subunit that were not obviously conserved [62,63] (Supplemental Figure S1A), and a large C- terminal truncation that removes the full Rpn13-binding region of Rpn2 [64–66] (Supplemental Figure S1B). This is consistent with the absence of an obvious Rpn13 ortholog in microsporidia, and together with the relatively poor conservation of known ubiquitin-binding residues on Rpn1 raises the possibility that Rpn10 may be the sole intrinsic ubiquitin receptor in this family of organisms.

With respect to the CP, all microsporidia species examined encoded at least 7 apparent α subunits and 7 apparent β subunits, consistent with other eukaryotes studied to date (Figure 1, Supplemental Table S2). Individual *N. ceranae* β subunits could be confidently matched to their orthologs using simple sequence homology searches. As is the case in *S. cerevisiae*, five of the seven β subunits appear to encode N-terminal propeptides that are anticipated to be cleaved during proteasome biogenesis, and the catalytic residues of the β1, β2, and β5 orthologs are readily identified (not shown and see below).

In contrast, individual α subunits could not be confidently matched to a particular ortholog upon pairwise sequence comparisons to α subunits of *S. cerevisiae* or humans. However, a structure-based homology search in combination with analysis of known distinguishing features of the yeast/human α ring permitted a reasonably confident identification of orthologs, and generation of a homology model of the *N. ceranae* α-ring built on the *S. cerevisiae* structure [67] (Supplemental Figure S2). Confidence in this model is supported by the presence of a conserved "pocket" lysine at the interfaces of all α subunit pairs except *N. ceranae* α1 and α7 (Supplemental Figure S2 and Table S3), as is the case in the human and yeast α rings. This lysine forms a salt bridge with the C-terminal carboxylate and/or a conserved tyrosine or phenylalanine residue of a particular Rpt subunit in the RP [68,69]. This tyrosine or phenylalanine is part of a so-called Hb-Y-X motif (where Hb is a hydrophobic residue and X is any amino acid), and is present in Rpt1, Rpt2, Rpt3, Rpt5, and Rpt6 in other eukaryotes. Docking of these Hb-Y-X motifs in turn opens a proteinaceous gate in the α ring, providing the substrate access to the CP peptidase sites for proteolysis [47,68,70]. Hb-Y-X motifs are similarly present at the C-termini of *N. ceranae* Rpt1, Rpt2, Rpt3, Rpt5, and Rpt6 (Rpt6 contains a hydrophobic residue but has a methionine in place of the tyrosine or phenylalanine). This suggests that a similar mechanism for gating is likely employed. However, the conserved YDR motif found in the N-termini of the α subunits of other eukaryotes that forms the gate of the CP [47,71] was notably absent in all seven *N. ceranae* subunits, suggesting an alternative structure of the proteinaceous gate.

We also searched for orthologs of the 11 known dedicated proteasome assembly chaperones, the proteasome modulator Blm10, and the proteasome-associated deubiquitinating enzyme Ubp6 (Supplemental Table S4). However, obvious orthologs for each of these, with the possible exception of Ubp6, were absent in virtually all microsporidia examined. These absences suggest potentially altered assembly and regulation of the proteasome in microsporidia, although it should be noted that the sequence conservation of some assembly chaperones is very weak even among other eukaryotes [72].

The biogenesis and function of the proteasome is highly regulated [73,74] via both transcriptional and post-translational mechanisms that control both the amount and activity of proteasome components [75]. The steady-state levels of the proteasome are tightly controlled in yeast [76,77], worms [78], flies [79], and mammals [80], although the mechanisms are distinct. In *S. cerevisiae*, expression of proteasome components is regulated by the transcription factor Rpn4, which binds to a 9 bp upstream activating sequence termed the proteasome-associated control element (PACE). Degradation of Rpn4 by the

proteasome [76,77] in turn serves as a direct method for conveying proteasome capacity information to the regulation of proteasome component gene expression by suppressing new proteasome subunit synthesis. Examination of the genomes of *N. ceranae* and other microsporidia revealed that these species do not possess obvious Rpn4 homologs, suggesting an altered mode of regulation of proteasome gene expression in these species. We also found no instances of the canonical PACE (GGTGGCAAA) in any of the CP or RP genes of *N. ceranae* (gene body +/− 500 bp of additional sequence examined, data not shown). It is important to note that while the Rpn4/PACE system is highly conserved in most fungi, it is not operative in some fungi, such as *S. pombe* [81], suggesting that novel mechanisms regulating proteasome component expression in fungi exist that could be important for microsporidia.

3.2. Proteasome Inhibition Controls Existing Infections by N. ceranae in Experimentally and Naturally Infected Bees

We wished to determine how proteasome inhibition would impact *N. ceranae* infection in honey bees. Many proteasome inhibitors are known to target the active site in 20S proteasome subunit β5 and its interface with 20S proteasome subunit β6 [82]. We first aligned the 20S proteasome subunit β5 homologs from *H. sapiens* (NP_002788.1), *A. mellifera* (XP_394680.3), *N. ceranae* (XP_024331353.1), *E. hellem* (XP_003887862.1), and *S. cerevisiae* (NP_015428.1). We found all three of the amino acids thought to be in catalytic triad (T1, D17, and K33 numbered from processed *H. sapiens* protein [83]) to be conserved. We also found a high degree of conservation for the amino acids critical for binding proteasome inhibitors (T2, R19, A20, T21, A22, G23, K33, A46, G47, G48, A49, A50, G129, S130, Y169, numbered from processed *H. sapiens* protein [82]) (Figure 2A). Other microsporidial β5 proteins possess similar levels of conservation (Supplemental Figure S3). We exploited the high sequence identity between β5 orthologs to produce a molecular model of the β5 subunit from *N. ceranae* bound to ixazomib, a modified peptide boronic acid that binds the β5 site of the 20 S proteasome and inhibits proteasome activity [84] (Figure 2B). In this model, no steric conflict between β5 and ixazomib was apparent, and many of the salt bridges and hydrogen bonds that stabilize the drug in the β5 active site were evident. Thus, we predicted that ixazomib, and likely many proteasome inhibitors, would bind to the β5 proteins in microsporidia and disrupt proteasome function.

Toward this goal, we first tested the ability of ixazomib to reduce *N. ceranae* infection in honey bees. After experimentally infecting bees collected from the landing board of an uninfected colony, we fed bees sucrose solution containing vehicle DMSO, 40 μM ixazomib, or 40 μM fumagillin for 4 days starting on 4 days post infection. On day 8 post infection, we then measured spore levels using light microscopy and the amounts of *N. ceranae β-actin* gene relative to honey bee *ATP5a* gene by qPCR (which allows measurement of all life stages of *N. ceranae* unlike spore counting) to determine the effects of proteasome inhibition on *N. ceranae* infection intensity. We found that feeding infected bees ixazomib for 96 h resulted in a dramatic reduction in infection intensity in infected bees by both measures (Figure 3A,B). Using bees from a highly infected colony (prevalence >90% infected), we fed bees sucrose solution containing vehicle DMSO, 40 μM ixazomib, or 40 μM fumagillin and observed a striking reduction in *N. ceranae* infection by both spore-counting and DNA analysis (Figure 3C,D).

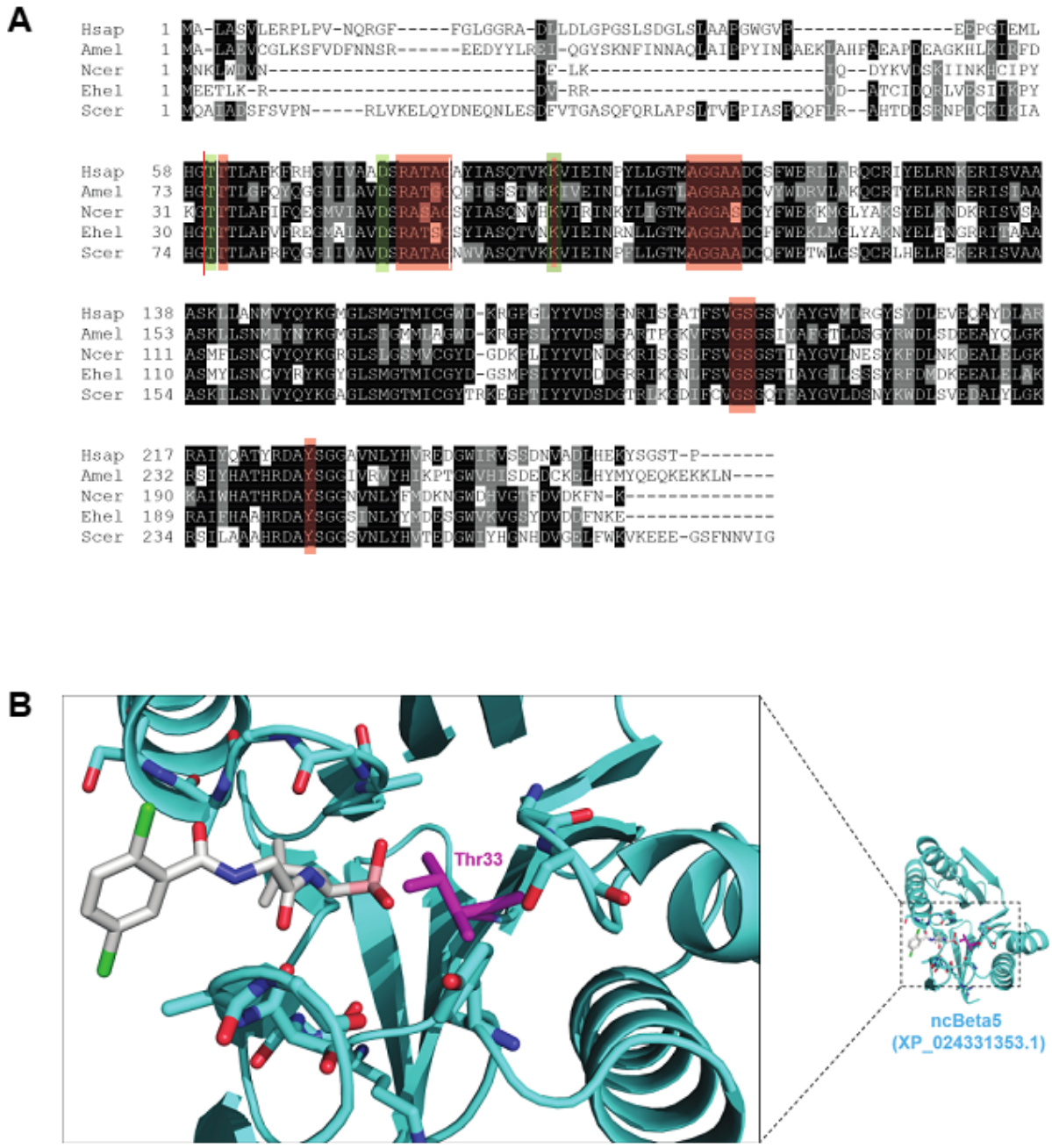

Figure 2. Conservation of key sequence and structural features of the β5 active site. (**A**) Sequence alignment of the 20S proteasome β5 subunit from *H. sapiens* (NP_002788.1), *A. mellifera* (XP_394680.3), *N. ceranae* (XP_024331353.1), *E. hellem* (XP_003887862.1), and *S. cerevisiae* (NP_015428.1). Amino acids from the catalytic triad (T1, D17, and K33 numbered from processed *H. sapiens* protein [83]) are boxed in green and amino acids critical for binding proteasome inhibitors (T2, R19, A20, T21, A22, G23, K33, A46, G47, G48, A49, A50, G129, S130, Y169, numbered from processed *H. sapiens* protein [82]) are boxed in red. The processing site for generating the mature protein is denoted with a red line. (**B**) Homology model of *N. ceranae* β5 bound to ixazomib. The β5 subunit is shown in ribbon mode. Residues forming electrostatic interactions with ixazomib in the crystal structure of ixazomib with the human CP are shown in stick mode, with the catalytic threonine colored magenta. Ixazomib is shown in stick mode with the boronate boron atom colored salmon.

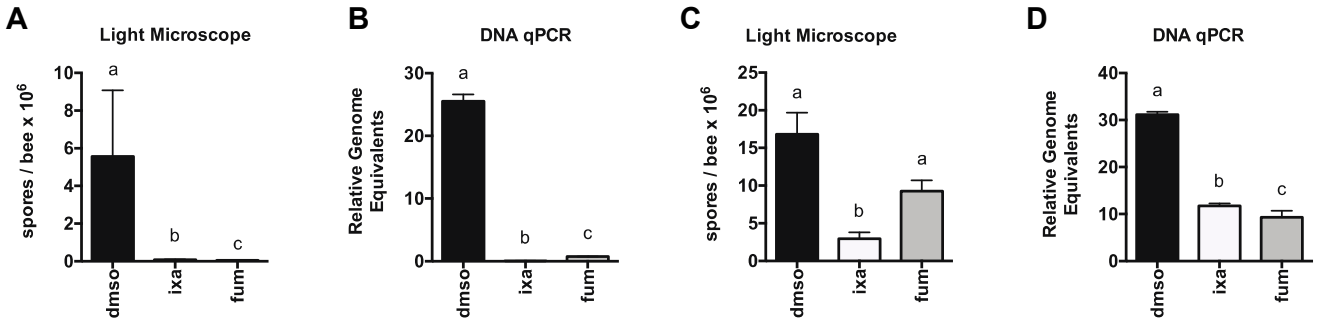

Figure 3. Proteasome inhibition reduces *N. ceranae* infection intensity in experimentally or naturally infected honey bees. *N. ceranae* levels in midguts as determined by spore count using light microscopy (**A**) or by qPCR (**B**) 8 days post infection in uninfected or infected landing board bees fed sucrose solution containing DMSO or ixazomib for the final 4 days. *N. ceranae* levels as determined by spore count using light microscopy (**C**) or by qPCR (**D**) in individual landing board bees from an infected colony captured and fed sucrose solution containing DMSO or ixazomib for 2 days, a $\neq$ b $\neq$ c, $p < 0.05$.

These results justified further testing of ixazomib and other proteasome inhibitors as possible anti-Nosema agents. Significant effort has been directed towards finding novel strategies for targeting the proteasome [85–87], providing a number of pharmacologic agents with varying efficacy, bioavailability, and selectivity. To standardize experiments by using age-matched bees and to allow for longer treatment periods, we used newly eclosed bees and tested the effects of a number of commercially available proteasome inhibitors, including ixazomib (MLN2238), ixazomib citrate (MLN9708), oprozomib (ONX 0912), dexazomib, carfilzomib, bortezomib, epoxomicin, HMB-Val-Ser-Leu-VE, MG262, and the two stereoisomers of MG132 (S and R) as well as fumagillin (Supplemental Table S5). On day 2 post-eclosion, *N. ceranae* spores (5×10^6/mL) were fed to bees in sucrose solution ad libitum [41] for 48 h. At 3 days post infection, honey bees in individual cages were fed sucrose solution containing one of the pharmacologic agents at 40 µM or vehicle control alone. For each trial, we individually tested two novel compounds simultaneously with an untreated group, a fumagillin treated group, and an ixazomib-treated group. After 4 days of drug feeding, honey bee midguts were dissected, and infection levels were assessed by spore counting and qPCR (Supplemental Figure S4). We observed reductions in infection level by relative genome equivalents for all tested proteasome inhibitors except HMB-Val-Ser-Leu-VE (Supplemental Figure S5 and Table S6). There were varying levels of impact on *N. ceranae* infection with ixazomib and its citrate salt being the most effective at reducing infection levels.

We focused on ixazomib and ixazomib citrate for further experiments. Again using newly eclosed bees, we treated infected bees for up to 8 days with sucrose solution containing vehicle DMSO, 40 µM ixazomib, or 40 µM fumagillin and measured infection level by spore counting and DNA on days 4 and 8 post initiation of treatment (Figure 4). We also looked at the dose responsiveness of ixazomib and ixazomib citrate on *N. ceranae* infection levels and observed a similar reduction in infection intensity at 10 µM and a diminished reduction in infection intensity at 2.5 µM of both ixazomib and ixazomib citrate by spore counting and DNA analysis (Figure 4C,D). Longer treatment periods did not result in greater decreases in *N. ceranae* infection intensity at doses <10 µM (data not shown).

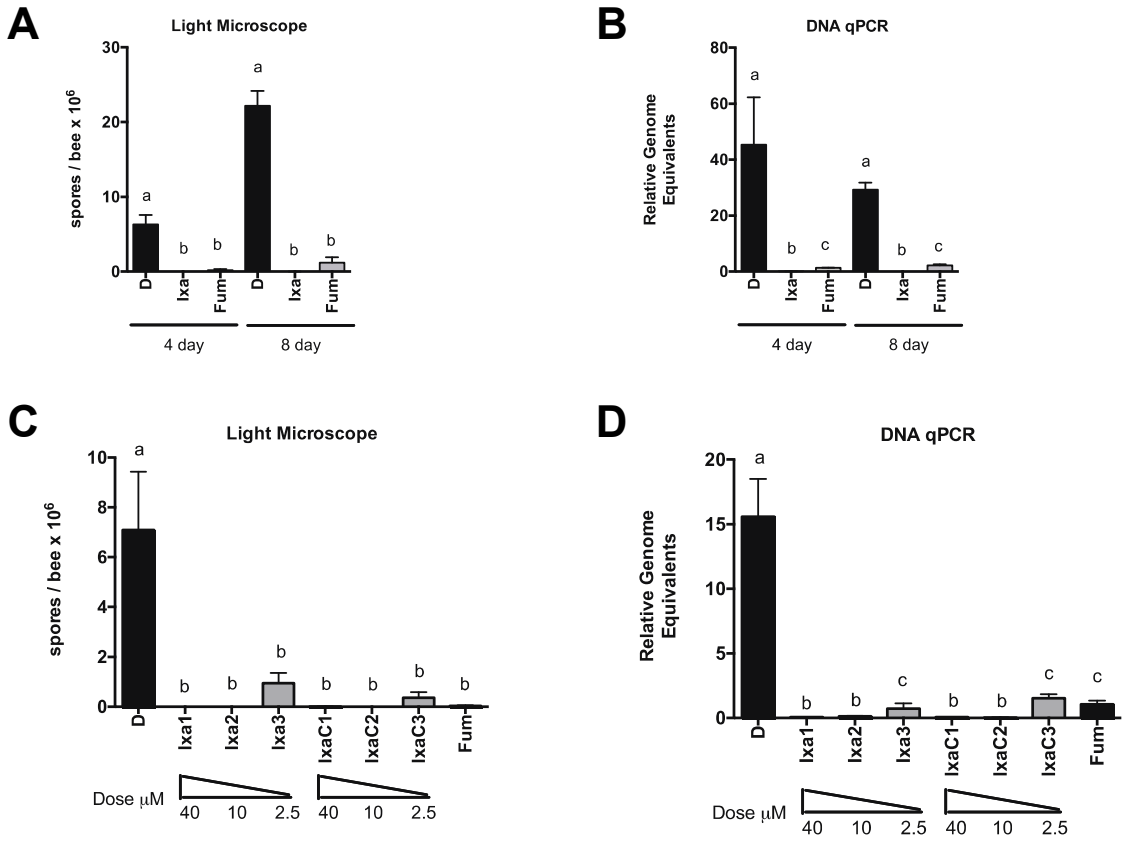

Figure 4. Ixazomib reduces *N. ceranae* infection level in a dose and time dependent manner in newly eclosed bees. (**A**) *N. ceranae* levels in midguts of infected newly eclosed bees fed sucrose solution containing DMSO or ixazomib for 4 or 8 days as determined by spore count using light microscopy (**A**) or by qPCR (**B**) a $\neq$ b, $p < 0.05$. *N. ceranae* levels in midguts of infected newly eclosed bees fed sucrose solution containing DMSO or various doses of ixazomib for 4 days as determined by spore count using light microscopy (**C**) or by qPCR (**D**) a $\neq$ b $\neq$ c, $p < 0.05$.

Finally, we wished to determine whether any rebound of *N. ceranae* infection was observed after cessation of treatment by ixazomib and ixazomib citrate as has been reported for fumagillin [18]. We treated infected newly eclosed bees with either sucrose solution containing ixazomib, ixazomib citrate, fumagillin, or vehicle alone for 4 days. We then switched all cages to sucrose solution alone for 4 days and then measured infection level by spore counting and DNA. We observed that infection intensity stayed. The same for bees receiving sucrose solution for the whole experiment, increased for those bees treated with fumagillin first, and decreased for those bees fed either ixazomib or ixazomib citrate first (Figure 5A,B). This suggested that even with a short treatment course, ixazomib and ixazomib citrate can eliminate infection with no evidence of subsequent reemergence. We found that the food consumed by newly eclosed bees did not differ by treatment and on the first day of drug feeding was 26.8 $\pm$ 4 μL per bee for 24 h. For 40 μM ixazomib (MW 361.03), this equals 0.39 μg consumed per day. If an adult honey bee is assumed to have a weight of 120 mg [88], then this results in an average of 0.39 mg/0.120 kg or 3.25 mg/kg per day for ixazomib.

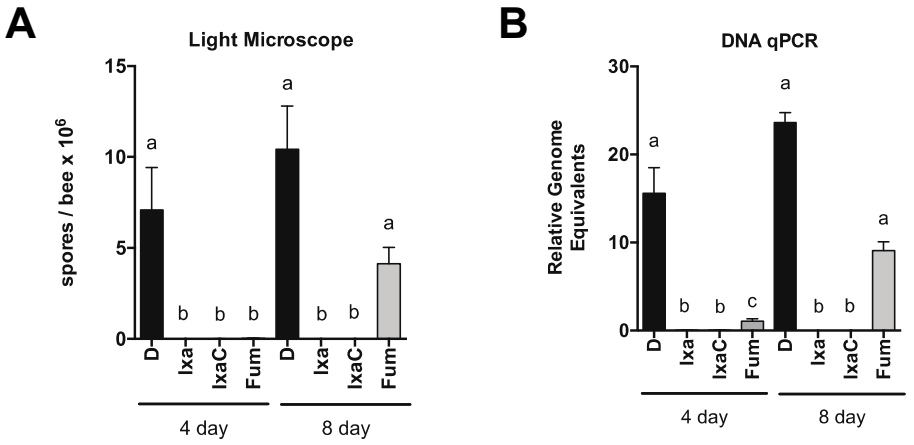

Figure 5. Ixazomib stably reduces *N. ceranae* infection in newly eclosed bees. *N. ceranae* levels in midguts of infected newly eclosed bees fed sucrose solution containing DMSO or ixazomib for 4 days before switching to DMSO alone, as determined by spore count using light microscopy (**A**) or by qPCR (**B**) a $\neq$ b, $p < 0.05$.

3.3. Honey Bee Survival Was Unaffected at Doses Up to 40-Fold Those Effective at Reducing N. ceranae Infection Intensity

To assess the impacts of ixazomib treatment on age-matched honey bees, newly emerged bees were fed sucrose solution containing ixazomib (40, 100, 200, 400, or 800 µM), fumagillin (at 40 µM), or vehicle alone for 10 days starting on 4 days post-eclosion. We found no deceased mortality of bees at 40, 100, or 200 µM of ixazomib. However, we observed decreased survival at 400 and 800 µM doses of ixazomib compared to bees fed sucrose solution containing vehicle alone (Figure 6).

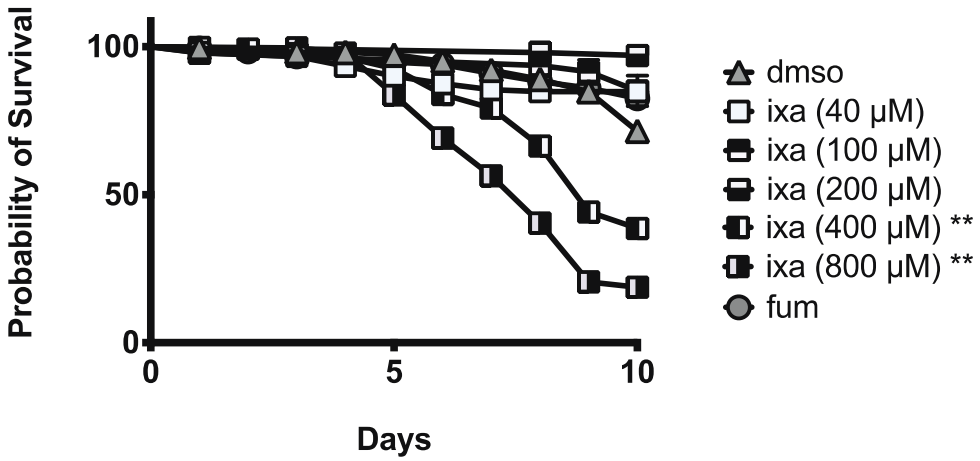

Figure 6. Ixazomib reduces honey bee survival at doses $\geq$ 40-fold above those that are effective at reducing *N. ceranae* infection intensity. Survival of individual honey bees fed sucrose solution (n = 368), fumagillin (40 µM, n = 366), or ixazomib (40 µM (n = 152), 100 µM (n = 47), 200 µM (n = 101), 400 µM (n = 391), 800 µM ixazomib (n = 282)). ** reduced survival relative to control with $p < 0.01$.

4. Discussion

Using a phylogenetic approach, we noted that the *N. ceranae* proteasome appears to lack multiple components observed in most eukaryotes, including multiple free-living fungal species. Examining the RP, we found that *N. ceranae* (and all microsporidia examined) are missing 4 of the 13 genes encoding Rpn subunits (*Rpn3*, *Rpn12*, *Rpn13*, and *Rpn15/Sem1*), and appear to lack at least one of the three known ubiquitin receptors on the proteasome, suggesting a simplified substrate recognition and/or processing mechanism. By contrast, we found that all microsporidia species examined have at least 7 CP α subunits and 7 CP

β subunits consistent with all other eukaryotes studied to date. This suggests that the CP is formed from two heteroheptameric α and two heteroheptameric β rings as is the case for other eukaryotes. Genes encoding proteasome assembly chaperones were not detected in *N. ceranae* or other microsporidia. It is important to note that microsporidia proteins are often extremely degenerate relative to their fungal counterparts and it is always formally possible that homologs were missed. *E. cuniculi* was originally thought to lack a gene for Sec61β, a component of the Sec translocon, but a highly divergent Sec61β gene was later discovered in microsporidia [89,90]. Although such chaperones may have gone undetected due to low sequence homology [72], it is also possible that the proteasomes in these organisms have evolved to assemble independent of exogenous chaperone activity. A detailed characterization of the composition and assembly of the microsporidian proteasome will be necessary to support this hypothesis.

We also found a striking reduction in *N. ceranae* infection intensity after pharmacological proteasome inhibition, as measured by spore counts and qPCR. Whereas all proteasome inhibitors had an effect, we found that ixazomib and its citrate salt had the largest effect on pathogen load. Different proteasome inhibitors have very different structures and modes of action within the proteasome [85–87]. Ixazomib is a modified peptide boronic acid that works by binding the catalytic site of the β5 subunit of the 20 S proteasome [82]. Ixazomib citrate (MLN9708), which is rapidly hydrolyzed under physiological conditions to its biologically active form, ixazomib (MLN2238), was the first orally bioavailable proteasome inhibitor, originally evaluated for the treatment of multiple myeloma [84]. Ixazomib citrate has demonstrated antitumor activity in a range of tumor xenograft models, as well as multiple myeloma models, and is now an FDA approved drug for multiple myeloma [91].

Targeting the UPS via pharmacologic inhibition of the proteasome [85–87] has now become a highly valuable strategy for treating numerous diseases. Of particular interest here, inhibition of proteasome function has been pursued in the treatment of infectious pathogens [92]. The protein degradation machinery is a valuable drug target in the context of other eukaryotic parasites, especially when it is possible to selectively target parasite proteasomes while sparing host proteasomes. The first proteasome inhibitors that were designed to preferentially inhibit eukaryotic pathogen proteasomes while sparing the host were discovered for malaria-causing *Plasmodium* spp. [93,94] and then the kinetoplastid parasites responsible for leishmaniasis, Chagas disease, and sleeping sickness [95]. Such a strategy could be highly valuable for *N. ceranae* treatment. Future studies that further characterize the structural and functional attributes of *N. ceranae* and other microsporidian proteasomes relative to the honey bee host proteasome could provide the basis for the pursuit of rational drug design to discover new proteasome inhibitors or modify existing inhibitors to develop novel compounds that optimize the efficacy to toxicity ratio.

There are a number of reasons why proteasome inhibition might be more toxic for the *N. ceranae* than the honey bee host. One possibility is that the proteasome inhibitors used in this study can preferentially inhibit the *N. ceranae* proteasome relative to that of the honey bee host. Alignment of the β5 subunit homologs from *N. ceranae* and select other species (including the honey bee) show high conservation of the critical ixazomib binding sites, suggesting that any selective inhibition does not occur via differences in this subunit. However, due to missing components (see above), the *N. ceranae* proteasome may have different functional attributes that make it more sensitive to inhibition relative to other eukaryotes. Further work will be required to examine this possibility.

Another reason may be a higher dependence on proteasome function in *N. ceranae* relative to the honey bee host. Microsporidia appear to have a high error rate in protein synthesis, with a high degree of amino acid substitutions in part due to changes in aminoacyl-tRNA synthetase structure [96]. This property may be compounded by the compacted ribosome found in microsporidia that is hypothesized to have reduced quality control function [97,98]. Whereas mistranslation may provide some benefits, such as functional diversity in proteins [96], it may come with costs such as a higher relative load of misfolded proteins that require degradation. We have hypothesized that gene loss

during genome compaction has led to reduced redundancy and flexibility to withstand cellular stresses [33]. A clear example of gene loss that would impact proteasome dependence occurs with autophagy, which represents another process involved in the clearance and degradation of proteins [99] with some overlap in function with the proteasome [36]. In other systems, proteasome inhibition often upregulates autophagy function [36], suggesting a compensatory role. Comparative genomics has revealed that microsporidia, like some protozoan parasites, have lost key molecular machinery involved in this process [100]. Thus, inability to rely on autophagy for protein degradation in the absence of proteasome inhibition likely makes this pharmacological disruption especially toxic to microsporidia cells.

Here, we hypothesize that proteasome inhibitors affect microsporidian cells directly by disruption of their proteasomes. It is also possible that the proteasome inhibitors impact the microsporidia indirectly through effects on the honey bee host proteasome [101]. For example, proteasome inhibition could induce a response in these cells that actively reduces *N. ceranae* infection. Two pieces of data argue against this possibility. First, proteasome inhibition has been shown to induce multiple cellular changes, including compensatory gene expression, through a proteasome regulatory network in other metazoans (reviewed in [102]). For example, in *D. melanogaster*, the transcription of select proteasome component genes is increased after genetic disruption of the proteasome [103]. We have shown that proteasome inhibition induces similar gene expression changes in the honey bee and these gene expression changes only occur at doses above those necessary for microsporidia reduction (manuscript in preparation). Second, the survival of the bees for up to 10 days at drug concentrations that are very toxic to *N. ceranae* suggests that proteasome function is not impacted to a dangerous level in the host at these doses. An additional potential mechanism for indirect effects involves the connection between the proteasome and anti-microsporidia immune pathways. One group has found that components responsible for ubiquitination, the proteasome, and autophagy are all important for defense against *N. parisii* infection in *C. elegans* [104]. However, proteasome inhibition would potentially allow for increased *N. ceranae* growth (instead of the observed decrease) if inhibition of the honey bee proteasome was the dominant effect.

When considering therapeutic strategies, it is also important to consider potential negative consequences of proteasome inhibition on honey bee health [101]. We observe that honey bees can tolerate doses of ixazomib up to levels ~40-fold above the concentration necessary to dramatically reduce *N. ceranae* infection (10 μM). This striking resistance to the proteotoxic stress caused by proteasome inhibition in honey bees might be expected. Due to their particular lifestyle, honey bees are exposed to significant routine thermal stress suggesting that the HSR might have unique properties in these insects. Colony-level homeostatic regulation of hive temperature is well recognized as an important adaptive feature of honey bees [105,106], which is maintained by complex individual behaviors, including endothermic shivering to increase heat ([107] and references therein). In maintaining this narrow range of hive temperature and in performing other specialized tasks such as foraging, the temperature of individual bees can increase significantly above steady-state to levels that would be dangerous to other organisms. For example, the temperatures of individual forager bees can reach up to 49 °C in flight [108]. However, honey bees appear highly resistant to thermal stress (reviewed in [109]), and possess a robust heat-shock response [110]. Such resilience may mean they have exceptional systems to combat the disruption in protein homeostasis caused by proteasome inhibitors. However, the impacts of ixazomib and ixazomib citrate (or other inhibitors described here) on individuals of different life stages and castes is not unknown. In particular, the impact on immature stages of bees, such as larvae and pupae will require close scrutiny. Studies in bees show that 20S proteasome activity decreases with aging in honey bee workers [111] although this decrease is not observed in queen bees [112]. Thus, the capacity of bees to withstand proteasome inhibition may differ with age. Perhaps even more obscure is the impact of proteasome inhibitors on overall colony health. Thus, a more comprehensive analysis of

the doses and long-term effects of such a treatment strategy on honey bee health, garnered through rigorous field trials, is imperative before they can be used in the management of *Nosema* infection [19].

In a related point, acquired resistance to any therapy is of concern. A recent study showed that *N. ceranae* infection loads eclipsed pre-treatment levels after cessation of fumagillin treatment through an unknown mechanism [18]. Our studies here in *N. ceranae* indicate that no rebound occurs after ixazomib treatment. However, our treatment period is short and we did not examine long-term outcomes at lower doses. Development of resistance in cancers treated with proteasome inhibitors occurs with some frequency. This is typically due to either mutations that disrupt drug binding to the proteasome or overexpression of catalytic β subunits that act as drug sinks [113], although other mechanisms are also possible [114]. Resistance to proteasome inhibitors has also been reported in treatment of infectious disease. For example, malaria parasites develop resistance to non-specific [115] and *Plasmodium*-specific [116] proteasome inhibitors through mutations that impact inhibitor binding. Thus, future studies to examine the stability of suppression and possible routes to resistance in *N. ceranae* should also be undertaken.

N. ceranae infection in honey bees can cause individual mortality and contribute to colony collapse. Infection can be treated with fumagillin, but due to concerns about efficacy, toxicity, and future availability, alternative therapeutic strategies are critical. *N. ceranae*, with a highly reduced genome, possesses an atypical proteasome lacking multiple components. We found that pharmacological proteasome inhibition led to a dramatic reduction in *N. ceranae* infection intensity without significant honey bee toxicity. These results suggest that proteasome inhibition can reduce microsporidia infection with limited toxicity to the honey bee host. While rigorous field trials will be required to assess the long-term effects of such a treatment strategy on honey bee health at the individual and colony level, our results offer a convincing novel treatment strategy for microsporidia infection in honey bees.

Supplementary Materials: The following are available online at https://www.mdpi.com/article/10.3390/biom11111600/s1, Figure S1: Comparisons of key Rpn1 and Rpn2 structural domains, Figure S2: *N. ceranae* α ring predictions, Figure S3: Sequence alignment of the 20S proteasome subunit β5 subunit from available microsporidia genomes, Figure S4: Schematic of *N. ceranae* infection of newly eclosed bees, Figure S5: Diverse proteasome inhibitors reduce *N. ceranae* infection in newly eclosed bees, Table S1: Predicted regulatory particle (RP) components, Table S2: Predicted Core Particle (CP) components, Table S3.: Summary of N. ceranae subunit sequence motifs predicted to mediate RP-CP interaction, Table S4: Predicted proteasome assembly components, Table S5: Commercially available proteasome inhibitors used in this study. Predicted proteasome assembly components, Table S6: Comparison of *N. ceranae* reduction versus control, fumagillin, and ixazomib. Video S1: Structural conservation of the *N. ceranae* proteasome.

Author Contributions: Conceptualization, R.J.T.J. and J.W.S.; methodology, R.J.T.J. and J.W.S.; software, R.J.T.J. and J.W.S.; validation, E.M.H., R.M.C., H.V.K., N.K.M.-B., R.J.T.J. and J.W.S.; formal analysis, E.M.H., R.M.C., H.V.K., N.K.M.-B., R.J.T.J. and J.W.S.; investigation, E.M.H., R.M.C., H.V.K., N.K.M.-B., R.J.T.J. and J.W.S.; resources, E.M.H., R.M.C., H.V.K., N.K.M.-B., R.J.T.J. and J.W.S.; data curation R.J.T.J. and J.W.S.; writing—original draft preparation, R.J.T.J. and J.W.S.; writing—review and editing, R.J.T.J. and J.W.S.; visualization, R.J.T.J. and J.W.S.; supervision, J.W.S.; project administration, J.W.S.; funding acquisition, R.J.T.J. and J.W.S. All authors have read and agreed to the published version of the manuscript.

Funding: This work is supported by the Agriculture and Food Research Initiative, Grant No. 2019-67030-29466/Project Accession No. 1019009 from the USDA National Institute of Food and Agriculture to J.W.S., by a generous grant from the California State Beekeepers Association to J.W.S., and NIH grant 5R01GM118600 to R.J.T.J.

Institutional Review Board Statement: Not applicable.

Informed Consent Statement: Not applicable.

Data Availability Statement: Not applicable.

Acknowledgments: We would also like to acknowledge Corey A. Marshalleck and Sun Graham for helpful comments and critical review of the manuscript.

Conflicts of Interest: The authors declare the following competing financial interest(s): J.W.S. is the inventor on US patent application no.16/597,836 filed by the Trustees of Columbia University in the City of New York, relating to compositions and methods for treatment of microsporidia infection using proteasome inhibitors.

References

1. Potts, S.G.; Imperatriz-Fonseca, V.; Ngo, H.T.; Aizen, M.A.; Biesmeijer, J.C.; Breeze, T.D.; Dicks, L.V.; Garibaldi, L.A.; Hill, R.; Settele, J.; et al. Safeguarding pollinators and their values to human well-being. *Nature* **2016**, *540*, 220–229. [CrossRef]
2. Goulson, D.; Nicholls, E.; Botías, C.; Rotheray, E.L. Bee declines driven by combined stress from parasites, pesticides, and lack of flowers. *Science* **2015**, *347*, 1255957. [CrossRef] [PubMed]
3. Evans, J.D.; Schwarz, R.S. Bees brought to their knees: Microbes affecting honey bee health. *Trends Microbiol.* **2011**, *19*, 614–620. [CrossRef] [PubMed]
4. Fries, I. Microsporidia, Honeybees, and Colony Collapse Disorder. *Microsporidia Pathog. Oppor.* **2014**, 571–577. [CrossRef]
5. Martín-Hernández, R.; Bartolomé, C.; Chejanovsky, N.; Le Conte, Y.; Dalmon, A.; Dussaubat, C.; García-Palencia, P.; Meana, A.; Pinto, M.A.; Soroker, V.; et al. Nosema ceranaein *Apis mellifera*: A 12 years postdetection perspective. *Environ. Microbiol.* **2018**, *20*, 1302–1329. [CrossRef] [PubMed]
6. Goblirsch, M. *Nosema ceranae* disease of the honey bee (*Apis mellifera*). *Apidologie* **2017**, *49*, 131–150. [CrossRef]
7. Higes, M.; Juarranz, Á.; Dias-Almeida, J.; Lucena, S.; Botías, C.; Meana, A.; García-Palencia, P.; Martín-Hernández, R. Apoptosis in the pathogenesis of Nosema ceranae (Microsporidia: *Nosematidae*) in honey bees (*Apis mellifera*). *Environ. Microbiol. Rep.* **2013**, *5*, 530–536. [CrossRef]
8. Higes, M.; García-Palencia, P.; Martín-Hernández, R.; Meana, A. Experimental infection of *Apis mellifera* honeybees with Nosema ceranae (Microsporidia). *J. Invertebr. Pathol.* **2007**, *94*, 211–217. [CrossRef]
9. Dussaubat, C.; Brunet, J.-L.; Higes, M.; Colbourne, J.K.; Lopez, J.; Choi, J.-H.; Martín-Hernández, R.; Botías, C.; Cousin, M.; Mcdonnell, C.; et al. Gut Pathology and Responses to the Microsporidium Nosema ceranae in the Honey Bee *Apis mellifera*. *PLoS ONE* **2012**, *7*, e37017. [CrossRef]
10. Alaux, C.; Crauser, D.; Pioz, M.; Saulnier, C.; Le Conte, Y. Parasitic and immune modulation of flight activity in honey bees tracked with optical counters. *J. Exp. Biol.* **2014**, *217*, 3416–3424. [CrossRef]
11. Goblirsch, M.; Huang, Z.Y.; Spivak, M. Physiological and Behavioral Changes in Honey Bees (*Apis mellifera*) Induced by Nosema ceranae Infection. *PLoS ONE* **2013**, *8*, e58165. [CrossRef]
12. Mayack, C.; Naug, D. Energetic stress in the honeybee *Apis mellifera* from Nosema ceranae infection. *J. Invertebr. Pathol.* **2009**, *100*, 185–188. [CrossRef]
13. Fries, I. Nosema ceranae in European honey bees (*Apis mellifera*). *J. Invertebr. Pathol.* **2010**, *103* (Suppl. 1), S73–S79. [CrossRef] [PubMed]
14. Lecocq, A.; Jensen, A.B.; Kryger, P.; Nieh, J.C. Parasite infection accelerates age polyethism in young honey bees. *Sci. Rep.* **2016**, *6*, 22042. [CrossRef]
15. Natsopoulou, M.E.; McMahon, D.P.; Paxton, R.J. Parasites modulate within-colony activity and accelerate the temporal polyethism schedule of a social insect, the honey bee. *Behav. Ecol. Sociobiol.* **2015**, *70*, 1019–1031. [CrossRef]
16. van den Heever, J.P.; Thompson, T.S.; Curtis, J.M.; Ibrahim, A.; Pernal, S.F. Fumagillin: An Overview of Recent Scientific Advances and Their Significance for Apiculture. *J. Agric. Food Chem.* **2014**, *62*, 2728–2737. [CrossRef]
17. Mendoza, Y.; Diaz-Cetti, S.; Ramallo, G.; Santos, E.; Porrini, M.; Invernizzi, C. Nosema ceranae Winter Control: Study of the Effectiveness of Different Fumagillin Treatments and Consequences on the Strength of Honey Bee (Hymenoptera: Apidae) Colonies. *J. Econ. Entomol.* **2017**, *110*, 1–5. [PubMed]
18. Huang, W.-F.; Solter, L.F.; Yau, P.M.; Imai, B.S. Nosema ceranae Escapes Fumagillin Control in Honey Bees. *PLoS Pathog.* **2013**, *9*, e1003185. [CrossRef]
19. Holt, H.L.; Grozinger, C.M. Approaches and Challenges to Managing Nosema (Microspora: *Nosematidae*) Parasites in Honey Bee (Hymenoptera: Apidae) Colonies. *J. Econ. Entomol.* **2016**, *109*, 1487–1503. [CrossRef] [PubMed]
20. Valizadeh, P.; Guzmán-Novoa, E.; Goodwin, P.H. Effect of Immune Inducers on Nosema ceranae Multiplication and Their Impact on Honey Bee (*Apis mellifera* L.) Survivorship and Behaviors. *Insects* **2020**, *11*, 572. [CrossRef]
21. Borges, D.; Guzmán-Novoa, E.; Goodwin, P.H. Effects of Prebiotics and Probiotics on Honey Bees (*Apis mellifera*) Infected with the Microsporidian Parasite Nosema ceranae. *Microorganisms* **2021**, *9*, 481. [CrossRef] [PubMed]
22. Nanetti, A.; Ugolini, L.; Cilia, G.; Pagnotta, E.; Malaguti, L.; Cardaio, I.; Matteo, R.; Lazzeri, L. Seed Meals from Brassica nigra and Eruca sativa Control Artificial Nosema ceranae Infections in *Apis mellifera*. *Microorganisms* **2021**, *9*, 949. [CrossRef]
23. Cilia, G.; Garrido, C.; Bonetto, M.; Tesoriero, D.; Nanetti, A. Effect of Api-Bioxal® and ApiHerb® Treatments against Nosema ceranae Infection in *Apis mellifera* Investigated by Two qPCR Methods. *Vet. Sci.* **2020**, *7*, 125. [CrossRef]
24. Porrini, M.P.; Garrido, P.M.; Umpiérrez, M.L.; Porrini, L.P.; Cuniolo, A.; Davyt, B.; González, A.; Eguaras, M.J.; Rossini, C. Effects of Synthetic Acaricides and Nosema ceranae (Microsporidia: *Nosematidae*) on Molecules Associated with Chemical Communication and Recognition in Honey Bees. *Vet. Sci.* **2020**, *7*, 199. [CrossRef] [PubMed]

25. Mura, A.; Pusceddu, M.; Theodorou, P.; Angioni, A.; Floris, I.; Paxton, R.J.; Satta, A. Propolis Consumption Reduces Nosema ceranae Infection of European Honey Bees (*Apis mellifera*). *Insects* **2020**, *11*, 124. [CrossRef]
26. Pașca, C.; Matei, I.A.; Diaconeasa, Z.; Rotaru, A.; Erler, S.; Dezmirean, D.S. Biologically Active Extracts from Different Medicinal Plants Tested as Potential Additives against Bee Pathogens. *Antibiotics* **2021**, *10*, 960. [CrossRef] [PubMed]
27. He, N.; Zhang, Y.; Duan, X.L.; Li, J.H.; Huang, W.-F.; Evans, J.D.; DeGrandi-Hoffman, G.; Chen, Y.P.; Huang, S.K. RNA Interference-Mediated Knockdown of Genes Encoding Spore Wall Proteins Confers Protection against Nosema ceranae Infection in the European Honey Bee, *Apis mellifera*. *Microorganisms* **2021**, *9*, 505. [CrossRef]
28. Borges, D.; Guzmán-Novoa, E.; Goodwin, P.H. Control of the microsporidian parasite Nosema ceranae in honey bees (*Apis mellifera*) using nutraceutical and immuno-stimulatory compounds. *PLoS ONE* **2020**, *15*, e0227484. [CrossRef]
29. Klassen, S.S.; VanBlyderveen, W.; Eccles, L.; Kelly, P.G.; Borges, D.; Goodwin, P.H.; Petukhova, T.; Wang, Q.; Guzmán-Novoa, E. Nosema ceranae Infections in Honey Bees (*Apis mellifera*) Treated with Pre/Probiotics and Impacts on Colonies in the Field. *Vet. Sci.* **2021**, *8*, 107. [CrossRef]
30. Burnham, A.J. Scientific Advances in Controlling Nosema ceranae (Microsporidia) Infections in Honey Bees (*Apis mellifera*). *Front. Vet. Sci.* **2019**, *6*, 810–818. [CrossRef] [PubMed]
31. Nakjang, S.; Williams, T.A.; Heinz, E.; Watson, A.K.; Foster, P.G.; Sendra, K.M.; Heaps, S.E.; Hirt, R.P.; Martin Embley, T. Reduction and Expansion in Microsporidian Genome Evolution: New Insights from Comparative Genomics. *Genome Biol. Evol.* **2013**, *5*, 2285–2303. [CrossRef]
32. McNamara-Bordewick, N.K.; McKinstry, M.; Snow, J.W. Robust Transcriptional Response to Heat Shock Impacting Diverse Cellular Processes despite Lack of Heat Shock Factor in Microsporidia. *mSphere* **2019**, *4*, e00219-19. [CrossRef]
33. Snow, J.W. Prolyl-tRNA synthetase inhibition reduces microsporidia infection intensity in honey bees. *Apidologie* **2020**, *51*, 557–569. [CrossRef]
34. Vilchez, D.; Saez, I.; Dillin, A. The role of protein clearance mechanisms in organismal ageing and age-related diseases. *Nat. Commun.* **2014**, *5*, 5659. [CrossRef]
35. Wolff, S.; Weissman, J.S.; Dillin, A. Differential scales of protein quality control. *Cell* **2014**, *157*, 52–64. [CrossRef]
36. Dikic, I. Proteasomal and Autophagic Degradation Systems. *Annu. Rev. Biochem.* **2017**, *86*, 193–224. [CrossRef] [PubMed]
37. Glickman, M.H.; Rubin, D.M.; Coux, O.; Wefes, I.; Pfeifer, G.; Cjeka, Z.; Baumeister, W.; Fried, V.A.; Finley, D. A subcomplex of the proteasome regulatory particle required for ubiquitin-conjugate degradation and related to the COP9-signalosome and eIF3. *Cell* **1998**, *94*, 615–623. [CrossRef]
38. Bard, J.A.M.; Goodall, E.A.; Greene, E.R.; Jonsson, E.; Dong, K.C.; Martin, A. Structure and Function of the 26S Proteasome. *Annu. Rev. Biochem.* **2018**, *87*, 697–724. [CrossRef]
39. Huang, W.-F.; Jiang, J.-H.; Chen, Y.-W.; Wang, C.-H. A Nosema ceranae isolate from the honeybee *Apis mellifera*. *Apidologie* **2007**, *38*, 30–37. [CrossRef]
40. Holt, H.L.; Aronstein, K.A.; Grozinger, C.M. Chronic parasitization by Nosema microsporidia causes global expression changes in core nutritional, metabolic and behavioral pathways in honey bee workers (*Apis mellifera*). *BMC Genom.* **2013**, *14*, 799. [CrossRef]
41. Fries, I.; Chauzat, M.-P.; Chen, Y.P.; Doublet, V.; Genersch, E.; Gisder, S.; Higes, M.; McMahon, D.P.; Martín-Hernández, R.; Natsopoulou, M.; et al. Standard methods for Nosema research. *J. Apic. Res.* **2013**, *52*, 1–28. [CrossRef]
42. Snow, J.W.; Ceylan Koydemir, H.; Karinca, D.K.; Liang, K.; Tseng, D.; Ozcan, A. Rapid imaging, detection, and quantification of Nosema ceranaespores in honey bees using mobile phone-based fluorescence microscopy. *Lab A Chip* **2019**, *19*, 789–797. [CrossRef] [PubMed]
43. Kanehisa, M.; Goto, S. KEGG: Kyoto encyclopedia of genes and genomes. *Nucleic Acids Res.* **2000**, *28*, 27–30. [CrossRef]
44. Johnston, B.A.; Hooks, K.B.; McKinstry, M.; Snow, J.W. Divergent forms of endoplasmic reticulum stress trigger a robust unfolded protein response in honey bees. *J. Insect Physiol.* **2016**, *86*, 1–10. [CrossRef]
45. Finley, D.; Ulrich, H.D.; Sommer, T.; Kaiser, P. The Ubiquitin-Proteasome System of Saccharomyces cerevisiae. *Genetics* **2012**, *192*, 319–360. [CrossRef]
46. Haag, K.L.; James, T.Y.; Pombert, J.-F.; Larsson, R.; Schaer, T.M.M.; Refardt, D.; Ebert, D. Evolution of a morphological novelty occurred before genome compaction in a lineage of extreme parasites. *Proc. Natl. Acad. Sci. USA* **2014**, *111*, 15480–15485. [CrossRef] [PubMed]
47. Eisele, M.R.; Reed, R.G.; Rudack, T.; Schweitzer, A.; Beck, F.; Nagy, I.; Pfeifer, G.; Plitzko, J.M.; Baumeister, W.; Tomko, R.J., Jr.; et al. Expanded Coverage of the 26S Proteasome Conformational Landscape Reveals Mechanisms of Peptidase Gating. *Cell Rep.* **2018**, *24*, 1301–1315.e5. [CrossRef] [PubMed]
48. Lander, G.C.; Estrin, E.; Matyskiela, M.E.; Bashore, C.; Nogales, E.; Martin, A. Complete subunit architecture of the proteasome regulatory particle. *Nature* **2012**, *482*, 186–191. [CrossRef]
49. Beck, F.; Unverdorben, P.; Bohn, S.; Schweitzer, A.; Pfeifer, G.; Sakata, E.; Nickell, S.; Plitzko, J.M.; Villa, E.; Baumeister, W.; et al. Near-atomic resolution structural model of the yeast 26S proteasome. *Proc. Natl. Acad. Sci. USA* **2012**, *109*, 14870–14875. [CrossRef] [PubMed]
50. Luan, B.; Huang, X.; Wu, J.; Mei, Z.; Wang, Y.; Xue, X.; Yan, C.; Wang, J.; Finley, D.J.; Shi, Y.; et al. Structure of an endogenous yeast 26S proteasome reveals two major conformational states. *Proc. Natl. Acad. Sci. USA* **2016**, *113*, 2642–2647. [CrossRef]

51. Unverdorben, P.; Beck, F.; Śledź, P.; Schweitzer, A.; Pfeifer, G.; Plitzko, J.M.; Baumeister, W.; Forster, F. Deep classification of a large cryo-EM dataset defines the conformational landscape of the 26S proteasome. *Proc. Natl. Acad. Sci. USA* **2014**, *111*, 5544–5549. [CrossRef]
52. Wehmer, M.; Rudack, T.; Beck, F.; Aufderheide, A.; Pfeifer, G.; Plitzko, J.M.; Förster, F.; Schulten, K.; Baumeister, W.; Sakata, E. Structural insights into the functional cycle of the ATPase module of the 26S proteasome. *Proc. Natl. Acad. Sci. USA* **2017**, *114*, 1305–1310. [CrossRef]
53. de la Peña, A.H.; Goodall, E.A.; Gates, S.N.; Lander, G.C.; Martin, A. Substrate-engaged 26 Sproteasome structures reveal mechanisms for ATP-hydrolysis–driven translocation. *Science* **2018**, *362*, eaav0725-11. [CrossRef]
54. Li, F.; Tian, G.; Langager, D.; Sokolova, V.; Finley, D.; Park, S. Nucleotide-dependent switch in proteasome assembly mediated by the Nas6 chaperone. *Proc. Natl. Acad. Sci. USA* **2017**, *114*, 1548–1553. [CrossRef] [PubMed]
55. Pathare, G.R.; Nagy, I.; Bohn, S.; Unverdorben, P.; Hubert, A.; Körner, R.; Nickell, S.; Lasker, K.; Sali, A.; Tamura, T.; et al. The proteasomal subunit Rpn6 is a molecular clamp holding the core and regulatory subcomplexes together. *Proc. Natl. Acad. Sci. USA* **2012**, *109*, 149–154. [CrossRef] [PubMed]
56. Nemec, A.A.; Peterson, A.K.; Warnock, J.L.; Reed, R.G.; Tomko, R.J., Jr. An Allosteric Interaction Network Promotes Conformation State-Dependent Eviction of the Nas6 Assembly Chaperone from Nascent 26S Proteasomes. *Cell Rep.* **2019**, *26*, 483–495.e5. [CrossRef] [PubMed]
57. Greene, E.R.; Goodall, E.A.; de la Peña, A.H.; Matyskiela, M.E.; Lander, G.C.; Martin, A. Specific lid-base contacts in the 26s proteasome control the conformational switching required for substrate degradation. *eLife* **2019**, *8*, 8626–8627. [CrossRef]
58. Estrin, E.; Lopez-Blanco, J.R.; Chacón, P.; Martin, A. Formation of an Intricate Helical Bundle Dictates the Assembly of the 26S Proteasome Lid. *Struct. Fold. Des.* **2013**, *21*, 1624–1635. [CrossRef]
59. Tomko, R.J., Jr.; Hochstrasser, M. Incorporation of the Rpn12 Subunit Couples Completion of Proteasome Regulatory Particle Lid Assembly to Lid-Base Joining. *Mol. Cell* **2011**, *44*, 907–917. [CrossRef]
60. Tomko, R.J., Jr.; Hochstrasser, M. The Intrinsically Disordered Sem1 Protein Functions as a Molecular Tether during Proteasome Lid Biogenesis. *Mol. Cell* **2014**, *53*, 433–443. [CrossRef] [PubMed]
61. Tomko, R.J., Jr.; Taylor, D.W.; Chen, Z.A.; Wang, H.-W.; Rappsilber, J.; Hochstrasser, M. A Single α Helix Drives Extensive Remodeling of the Proteasome Lid and Completion of Regulatory Particle As-sembly. *Cell* **2015**, *163*, 432–444. [CrossRef] [PubMed]
62. Shi, Y.; Chen, X.; Elsasser, S.; Stocks, B.B.; Tian, G.; Lee, B.-H.; Shi, Y.; Zhang, N.; de Poot, S.A.H.; Tuebing, F.; et al. Rpn1 provides adjacent receptor sites for substrate binding and deubiquitination by the proteasome. *Science* **2016**, *351*, aad9421. [CrossRef]
63. Boughton, A.J.; Liu, L.; Lavy, T.; Kleifeld, O.; Fushman, D. A novel recognition site for polyubiquitin and ubiquitin-like signals in an unexpected region of proteasomal subunit Rpn1. *J. Biol. Chem.* **2021**, *297*, 101052. [CrossRef] [PubMed]
64. VanderLinden, R.T.; Hemmis, C.W.; Yao, T.; Robinson, H.; Hill, C.P. Structure and energetics of pairwise interactions between proteasome subunits RPN2, RPN13, and ubiquitin clarify a substrate recruitment mechanism. *J. Biol. Chem.* **2017**, *292*, 9493–9504. [CrossRef] [PubMed]
65. Lu, X.; Nowicka, U.; Sridharan, V.; Liu, F.; Randles, L.; Hymel, D.; Dyba, M.; Tarasov, S.G.; Tarasova, N.I.; Zhao, X.Z.; et al. Structure of the Rpn13-Rpn2 complex provides insights for Rpn13 and Uch37 as anticancer targets. *Nat. Commun.* **2017**, *8*, 15540. [CrossRef] [PubMed]
66. Lu, X.; Ebelle, D.L.; Matsuo, H.; Walters, K.J. An Extended Conformation for K48 Ubiquitin Chains Revealed by the hRpn2:Rpn13:K48-Diubiquitin Structure. *Struct. Fold. Des.* **2020**, *28*, 495–506.e3. [CrossRef]
67. Groll, M.; Ditzel, L.; Lowe, J.; Stock, D.; Bochtler, M.; Bartunik, H.D.; Huber, R. Structure of 20S proteasome from yeast at 2.4 angstrom resolution. *Nature* **1997**, *386*, 463–471. [CrossRef]
68. Smith, D.M.; Chang, S.-C.; Park, S.; Finley, D.; Cheng, Y.; Goldberg, A.L. Docking of the Proteasomal ATPases" Carboxyl Termini in the 20S Proteasome"s α Ring Opens the Gate for Substrate Entry. *Mol. Cell* **2007**, *27*, 731–744. [CrossRef]
69. Yu, Y.; Smith, D.M.; Kim, H.M.; Rodriguez, V.; Goldberg, A.L.; Cheng, Y. Interactions of PAN's C-termini with archaeal 20S proteasome and implications for the eukaryotic proteasome-ATPase interactions. *EMBO J.* **2010**, *29*, 692–702. [CrossRef]
70. Rabl, J.; Smith, D.M.; Yu, Y.; Chang, S.-C.; Goldberg, A.L.; Cheng, Y. Mechanism of Gate Opening in the 20S Proteasome by the Proteasomal ATPases. *Mol. Cell* **2008**, *30*, 360–368. [CrossRef]
71. Groll, M.; Bajorek, M.; Köhler, A.; Moroder, L.; Rubin, D.M.; Huber, R.; Glickman, M.H.; Finley, D. A gated channel into the proteasome core particle. *Nat. Struct. Biol.* **2000**, *7*, 1062–1067. [CrossRef]
72. Funakoshi, M.; Tomko, R.J., Jr.; Kobayashi, H.; Hochstrasser, M. Multiple Assembly Chaperones Govern Biogenesis of the Proteasome Regulatory Particle Base. *Cell* **2009**, *137*, 887–899. [CrossRef]
73. Howell, L.A.; Tomko, R.J.; Kusmierczyk, A.R. Putting it all together: Intrinsic and extrinsic mechanisms governing proteasome biogenesis. *Front. Biol.* **2017**, *12*, 19–48. [CrossRef]
74. Livneh, I.; Cohen-Kaplan, V.; Cohen-Rosenzweig, C.; Avni, N.; Ciechanover, A. The life cycle of the 26S proteasome: From birth, through regulation and function, and onto its death. *Cell Res.* **2016**, *26*, 869–885. [CrossRef] [PubMed]
75. Collins, G.A.; Goldberg, A.L. The Logic of the 26S Proteasome. *Cell* **2017**, *169*, 792–806. [CrossRef] [PubMed]
76. Xie, Y.M.; Varshavsky, A. RPN4 is a ligand, substrate, and transcriptional regulator of the 26S proteasome: A negative feedback circuit. *Proc. Natl. Acad. Sci. USA* **2001**, *98*, 3056–3061. [CrossRef] [PubMed]

77. Mannhaupt, G.; Schnall, R.; Karpov, V.; Vetter, I.; Feldmann, H. Rpn4p acts as a transcription factor by binding to PACE, a nonamer box found upstream of 26S proteasomal and other genes in yeast. *FEBS Lett.* **1999**, *450*, 27–34. [CrossRef]
78. Li, X.; Matilainen, O.; Jin, C.; Glover-Cutter, K.M.; Holmberg, C.I.; Blackwell, T.K. Specific SKN-1/Nrf Stress Responses to Perturbations in Translation Elongation and Proteasome Activity. *PLoS Genet.* **2011**, *7*, e1002119-14. [CrossRef]
79. Szlanka, T.; Haracska, L.; Kiss, I.; Deák, P.; Kurucz, E.; Andó, I.; Virágh, E.; Udvardy, A. Deletion of proteasomal subunit S5a/Rpn10/p54 causes lethality, multiple mitotic defects and overexpression of proteasomal genes in Drosophila melanogaster. *J. Cell Sci.* **2003**, *116*, 1023–1033. [CrossRef]
80. Meiners, S.; Heyken, D.; Weller, A.; Ludwig, A.; Stangl, K.; Kloetzel, P.-M.; Krüger, E. Inhibition of proteasome activity induces concerted expression of proteasome genes and de novo formation of Mammalian proteasomes. *J. Biol. Chem.* **2003**, *278*, 21517–21525. [CrossRef] [PubMed]
81. Mannhaupt, G.; Feldmann, H. Genomic Evolution of the Proteasome System Among Hemiascomycetous Yeasts. *J. Mol. Evol.* **2007**, *65*, 529–540. [CrossRef] [PubMed]
82. Schrader, J.; Henneberg, F.; Mata, R.A.; Tittmann, K.; Schneider, T.R.; Stark, H.; Bourenkov, G.; Chari, A. The inhibition mechanism of human 20S proteasomes enables next-generation inhibitor design. *Science* **2016**, *353*, 594–598. [CrossRef] [PubMed]
83. Huber, E.M.; Heinemeyer, W.; Li, X.; Arendt, C.S.; Hochstrasser, M.; Groll, M. A unified mechanism for proteolysis and autocatalytic activation in the 20S proteasome. *Nat. Commun.* **2016**, *7*, 10900–10910. [CrossRef]
84. Kupperman, E.; Lee, E.C.; Cao, Y.; Bannerman, B.; Fitzgerald, M.; Berger, A.; Yu, J.; Yang, Y.; Hales, P.; Bruzzese, F.; et al. Evaluation of the Proteasome Inhibitor MLN9708 in Preclinical Models of Human Cancer. *Cancer Res.* **2010**, *70*, 1970–1980. [CrossRef]
85. Goldberg, A.L. Development of proteasome inhibitors as research tools and cancer drugs. *J. Cell Biol.* **2012**, *199*, 583–588. [CrossRef]
86. Śledź, P.; Baumeister, W. Structure-Driven Developments of 26S Proteasome Inhibitors. *Annu. Rev. Pharmacol. Toxicol.* **2016**, *56*, 191–209. [CrossRef] [PubMed]
87. Cromm, P.M.; Crews, C.M. The Proteasome in Modern Drug Discovery: Second Life of a Highly Valuable Drug Target. *ACS Cent. Sci.* **2017**, *3*, 830–838. [CrossRef]
88. Hrassnigg, N.; Crailsheim, K. Differences in drone and worker physiology in honeybees (*Apis mellifera*). *Apidologie* **2005**, *36*, 255–277. [CrossRef]
89. Slamovits, C.H.; Burri, L.; Keeling, P.J. Characterization of a Divergent Sec61β Gene in Microsporidia. *J. Mol. Biol.* **2006**, *359*, 1196–1202. [CrossRef]
90. WU, Z.; LI, Y.; Pan, G.; Li, C.; HU, J.; LIU, H.; Zhou, Z.; Xiang, Z. A Complete Sec61 Complex in Nosema Bombycis and Its Comparative Genomics Analyses. *J. Eukaryot. Microbiol.* **2007**, *54*, 379–380. [CrossRef]
91. Azab, A.K.; Muz, B.; Ghazarian, R.; Ou, M.; Luderer, M.; Kusdono, H. Spotlight on ixazomib: Potential in the treatment of multiple myeloma. *Drug Des. Dev. Ther.* **2016**, *10*, 217. [CrossRef]
92. Bibo-Verdugo, B.; Jiang, Z.; Caffrey, C.R.; O'Donoghue, A.J. Targeting proteasomes in infectious organisms to combat disease. *FEBS J.* **2017**, *284*, 1503–1517. [CrossRef] [PubMed]
93. Li, H.; O'Donoghue, A.J.; van der Linden, W.A.; Xie, S.C.; Yoo, E.; Foe, I.T.; Tilley, L.; Craik, C.S.; da Fonseca, P.C.A.; Bogyo, M. Structure- and function-based design of Plasmodium-selective proteasome inhibitors. *Nature* **2016**, *530*, 233–236. [CrossRef]
94. LaMonte, G.M.; Almaliti, J.; Bibo-Verdugo, B.; Keller, L.; Zou, B.Y.; Yang, J.; Antonova-Koch, Y.; Orjuela-Sanchez, P.; Boyle, C.A.; Vigil, E.; et al. Development of a Potent Inhibitor of the Plasmodium Proteasome with Reduced Mammalian Toxicity. *J. Med. Chem.* **2017**, *60*, 6721–6732. [CrossRef] [PubMed]
95. Khare, S.; Nagle, A.S.; Biggart, A.; Lai, Y.H.; Liang, F.; Davis, L.C.; Barnes, S.W.; Mathison, C.J.N.; Myburgh, E.; Gao, M.-Y.; et al. Proteasome inhibition for treatment of leishmaniasis, Chagas disease and sleeping sickness. *Nature* **2016**, *537*, 229–233. [CrossRef]
96. Melnikov, S.V.; Rivera, K.D.; Ostapenko, D.; Makarenko, A.; Sanscrainte, N.D.; Becnel, J.J.; Solomon, M.J.; Texier, C.; Pappin, D.J.; Söll, D. Error-prone protein synthesis in parasites with the smallest eukaryotic genome. *Proc. Natl. Acad. Sci. USA* **2018**, *115*, E6245–E6253. [CrossRef] [PubMed]
97. Melnikov, S.; Manakongtreecheep, K.; Rivera, K.; Makarenko, A.; Pappin, D.; Söll, D. Muller's Ratchet and Ribosome Degeneration in the Obligate Intracellular Parasites Microsporidia. *Int. J. Mol. Sci.* **2018**, *19*, 4125. [CrossRef]
98. Barandun, J.; Hunziker, M.; Vossbrinck, C.R.; Klinge, S. Evolutionary compaction and adaptation visualized by the structure of the dormant microsporidian ribosome. *Nat. Microbiol.* **2019**, *4*, 1798–1804. [CrossRef]
99. Reggiori, F.; Klionsky, D.J. Autophagic Processes in Yeast: Mechanism, Machinery and Regulation. *Genetics* **2013**, *194*, 341–361. [CrossRef]
100. Duszenko, M.; Ginger, M.L.; Brennand, A.; Gualdrón-López, M.; Colombo, M.I.; Coombs, G.H.; Coppens, I.; Jayabalasingham, B.; Langsley, G.; Lisboa de Castro, S.; et al. Autophagy in protists. *Autophagy* **2014**, *7*, 127–158. [CrossRef]
101. Schmidt, M.; Finley, D. Biochimica et Biophysica Acta. *BBA-Mol. Cell Res.* **2014**, *1843*, 13–25.
102. Albornoz, N.; Bustamante, H.; Soza, A.; Burgos, P. Cellular Responses to Proteasome Inhibition: Molecular Mechanisms and Beyond. *Int. J. Mol. Sci.* **2019**, *20*, 3379. [CrossRef] [PubMed]
103. Lundgren, J.; Masson, P.; Mirzaei, Z.; Young, P. Identification and Characterization of a Drosophila Proteasome Regulatory Network. *Mol. Cell Biol.* **2005**, *25*, 4662–4675. [CrossRef]

104. Bakowski, M.A.; Desjardins, C.A.; Smelkinson, M.G.; Dunbar, T.L.; Dunbar, T.A.; Lopez-Moyado, I.F.; Rifkin, S.A.; Cuomo, C.A.; Troemel, E.R. Ubiquitin-mediated response to microsporidia and virus infection in C. elegans. *PLoS Pathog.* **2014**, *10*, e1004200. [CrossRef]
105. Seeley, T.D. *Honeybee Ecology: A Study of Adaptation in Social Life*; Princeton Univ. Press: Princeton, NJ, USA, 1985.
106. Heinrich, B. *The Hot-Blooded Insects*; Harvard University Press: Cambridge, MA, USA, 1993.
107. Heinrich, B.; Seeley, T.D. Regulation of temperature in the nests of social insects. In *Insect Thermoregulation*; Heinrich, B., Ed.; John WIley and Sons: New York, NY, USA, 1981.
108. Elekonich, M.M.; Roberts, S.P. Honey bees as a model for understanding mechanisms of life history transitions. *Comp. Biochem. Physiol. Part A Mol. Integr. Physiol.* **2005**, *141*, 362–371. [CrossRef] [PubMed]
109. Abou-Shaara, H.F.; Owayss, A.A.; Ibrahim, Y.Y.; Basuny, N.K. A review of impacts of temperature and relative humidity on various activities of honey bees. *Insect. Soc.* **2017**, *64*, 455–463. [CrossRef]
110. McKinstry, M.; Chung, C.; Truong, H.; Johnston, B.A.; Snow, J.W. The heat shock response and humoral immune response are mutually antagonistic in honey bees. *Sci. Rep.* **2017**, *7*, 8850. [CrossRef]
111. Hsu, C.-Y.; Chuang, Y.-L.; Chan, Y.-P. Changes in cellular degradation activity in young and old worker honeybees (*Apis mellifera*). *Exp. Gerontol.* **2014**, *50*, 128–136. [CrossRef]
112. Hsu, C.-Y.; Qiu, J.T.; Chan, Y.-P. Cellular degradation activity is maintained during aging in long-living queen bees. *Biogerontology* **2016**, *17*, 829–840. [CrossRef]
113. Oerlemans, R.; Franke, N.E.; Assaraf, Y.G.; Cloos, J.; van Zantwijk, I.; Berkers, C.R.; Scheffer, G.L.; Debipersad, K.; Vojtekova, K.; Lemos, C.; et al. Molecular basis of bortezomib resistance: Proteasome subunit β5 (PSMB5) gene mutation and overexpression of PSMB5 protein. *Blood* **2008**, *112*, 2489–2499. [CrossRef]
114. Farrell, M.L.; Reagan, M.R. Soluble and Cell–Cell-Mediated Drivers of Proteasome Inhibitor Resistance in Multiple Myeloma. *Front. Endocrinol.* **2018**, *9*, 561–567. [CrossRef] [PubMed]
115. Xie, S.C.; Gillett, D.L.; Spillman, N.J.; Tsu, C.; Luth, M.R.; Ottilie, S.; Duffy, S.; Gould, A.E.; Hales, P.; Seager, B.A.; et al. Target Validation and Identification of Novel Boronate Inhibitors of the Plasmodium falciparum Proteasome. *J. Med. Chem.* **2018**, *61*, 10053–10066. [CrossRef] [PubMed]
116. Kirkman, L.A.; Zhan, W.; Visone, J.; Dziedziech, A.; Singh, P.K.; Fan, H.; Tong, X.; Bruzual, I.; Hara, R.; Kawasaki, M.; et al. Antimalarial proteasome inhibitor reveals collateral sensitivity from intersubunit interactions and fitness cost of resistance. *Proc. Natl. Acad. Sci. USA* **2018**, *115*, E6863–E6870. [CrossRef] [PubMed]